Collective Flows in High-Energy Heavy-Ion Collisions from AGS to SPS

A. Ohnishi[1], M. Isse[1], N. Otuka[2], P. K. Sahu[3], Y. Nara[4]

[1] *Division of Physics, Graduate School of Science, Hokkaido University*
[2] *Nuclear Data Center, Department of Nuclear Energy System, JAERI*
[3] *Institute of Physics, Bhubaneswar, India*
[4] *Department of Physics, University of Arizona, USA*

Abstract

Collective flows in heavy-ion collisions from SIS (1 A GeV), AGS (2-11 A GeV) to SPS (158 A GeV) energies are investigated in a transport model with mean-field. Calculated results with momentum dependent mean-field qualitatively reproduce the experimental data of sideward, directed, and elliptic flows in this incident energy range.

1 Introduction

Determining the nuclear equation of state (EOS) under various conditions has been one of the largest motivations of nuclear physics in these decades [1]. At around the saturation density, EOS gives the bulk properties of nuclei such as the binding energy and the radius. EOS of asymmetric nuclear matter ($N \gg Z$) is crucial in understanding the compositions in neutron stars, and it may be probed through the study of neutron rich nuclei. At high densities, hadrons with strangeness such as hyperons and kaons may emerge, and the interactions of these particles in nuclear matter has becomes clearer in recent strangeness nuclear physics. In high-energy heavy-ion collisions, where nuclear matter in a wide of range of temperatures and densities are probed, many ideas on EOS and phases have been examined. For example, the gas of deconfined quarks and gluons (QGP) seems to be created in recent RHIC experiments.

Compared to hot baryon-free nuclear matter, for which the first principle lattice QCD simulations are possible [2], roles of experimental information and related phenomenological studies are more important for the study of nuclear matter at high baryon densities. In 1980's, the existence of strong collective flow in heavy-ion collisions was suggested in hydrodynamics [3, 4], and it was examined in experiments at Bevalac [5]. Collective sideward flows are generated in the early stage of collisions by the repulsive nucleon potential in nuclear matter, then the observed strong collective flows were believed to signal very large pressure at high baryon densities, i.e. hard EOS [1, 6]. At high incident energies, however, the real part of the nucleon-nucleus potential is already repulsive at the normal density, then the role of this momentum dependence of nuclear potential on the collective flows were extensively studied from around 1990 [7, 8, 9]. In order to distinguish the momentum and density dependence, we need to invoke heavy-ion collision data in a wide incident energy range. We have now systematic collective flow data at various incident energies; LBNL-Bevalac [12, 13, 14], GSI-SIS [15, 16], BNL-AGS [17, 18, 19, 20], CERN-SPS [21, 22, 23], and BNL-RHIC.

Collective flow data obtained at AGS energies ($2 - 11A$ GeV) show a good landmark to determine EOS. In order to explain all of the radial, sideward, and elliptic flows at AGS energies, it is necessary to take care of the saturating momentum dependence of the mean-field and increasing resonance and string degrees of freedom [24]. More recently, Danielewicz et al. have discussed EOS with these data by Boltzmann transport based mean-field model [9, 10, 11], showing that while softer EOS ($K \sim 167$ MeV) is preferred at low incident energies, we need stiffer EOS ($K \sim 300$ MeV) at higher AGS energies. Finally, they have concluded that the allowed pressure range as a function of baryon density ($\rho_B = (2-4.5)\rho_0$) is constraint by experiments. While their analysis is systematic and extensive, it would be still premature to obtain the final conclusion. For sideward flow, results with RBUU [24] give a better description in a relativistic mean-field with a momentum cut off for the meson-baryon coupling. In addition, we still have a large ambiguity in the mean-field for hadrons other than nucleons. In order to reduce these ambiguities and to pin down the EOS more precisely, recently measured flow data at lower SPS energies ($20 - 80A$ GeV) would be helpful, because the highest baryon density is expected be reached at around $E_{\rm inc} \sim 20 - 40A$ GeV and the mean-field effects on collective flows have not been seriously investigated at this energy regime.

In this work, we investigate collective flows from 1 A GeV to 160 A GeV by using a hadronic cascade model (JAM) [25] combined with a covariant prescription of mean-field (RQMD/S) [26].

2 Model of EOS Study in High-Energy Heavy-Ion Collisions

Heavy-ion collision is a dynamical process of a system in which the temperature and density are not uniform and the equilibrium is not necessarily reached. Then we need dynamical models to describe collisions in order to extract static properties of nuclear matter under equilibrium. Hydrodynamical description is the most direct way to connect the EOS and dynamics. Actually, hydrodynamics has succeeded at RHIC, where the number of produced particles is so large that local equilibrium is easily achieved. However the condition of local equilibrium may not be satisfied up to SPS energies, then non-equilibrium dynamics is required to obtain the EOS of dense nuclear matter. In this work, we apply a combined framework of hadron-string cascade JAM [25], and covariant constraint Hamiltonian dynamics RQMD/S [26].

Hadron-string cascade is the main source of thermalization and particle production up to SPS energies. In the energy range of $E_{\rm inc} = 1 - 160A$ GeV, main particle production mechanism in hadron-hadron collisions evolves from resonance production to string formation. At higher energies, partonic interaction (jet production) becomes more important, and the jet production cross section reaches around 20 % of the total cross section of pp at RHIC [27].

In JAM [25], all of the above particle production mechanisms are included, then the applicable incident energy range is expected to be wide. Inelastic hadron-hadron collisions produce resonances at low energies. We explicitly include all established hadronic states with masses up to around 2 GeV with explicit isospin states as well as their antiparticles, which are made to propagate in space-time. At higher energies ($\sqrt{s} \gtrsim 4$ GeV in BB collisions, $\sqrt{s} \gtrsim 3$ GeV in MB collisions, and $\sqrt{s} \gtrsim 2$ GeV in MM collisions), color strings are formed and they decay into hadrons after their formation time ($\tau \sim 1$ fm/c) according to the Lund string model PYTHIA [32]. Hadrons which have original constituent quarks can scatter with other hadrons assuming the additive quark cross section within a formation time. This simulates string-hadron collisions which is known to be important at SPS energies. At high energies ($\sqrt{s} \gtrsim 10$ GeV), multiple mini-jet production is also included in the same way as the HIJING model [27] in which jet cross section and the number of jet are calculated using an eikonal formalism for perturbative QCD. Hard parton-parton scattering with initial and final state radiation are simulated using PYTHIA [32].

While the particle production yield and momentum distribution are reasonably well reproduced in cascade models, it is necessary to include mean-field effects to explain collective flow data. In order to describe the flow data in a wide energy range, the mean-field should have the momentum dependence as well as the density dependence. We adopt here a simple Skyrme type density dependent mean-field in the zero-range approximation, and a Lorentzian type momentum dependent mean-field which simulates the exchange term (Fock term) of the Yukawa potential as follows,

$$U(\boldsymbol{r},\boldsymbol{p}) = \alpha\left(\frac{\rho(\boldsymbol{r})}{\rho_0}\right) + \beta\left(\frac{\rho(\boldsymbol{r})}{\rho_0}\right)^{\gamma} + \sum_{k=1}^{2}\frac{C_{\rm ex}^{(k)}}{\rho_0}\int d\boldsymbol{p}'\frac{f(\boldsymbol{r},\boldsymbol{p}')}{1+[(\boldsymbol{p}-\boldsymbol{p}')/\mu_k]^2}\ . \tag{1}$$

This mean-field potential leads to the following total potential energy,

$$V = \int d\boldsymbol{r}\left[\frac{\alpha\rho^2(\boldsymbol{r})}{2\rho_0} + \frac{\beta\rho^{\gamma+1}(\boldsymbol{r})}{(1+\gamma)\rho_0^{\gamma}}\right] + \sum_{k=1}^{2}\frac{C_{\rm ex}^{(k)}}{2\rho_0}\int d\boldsymbol{r}d\boldsymbol{p}d\boldsymbol{p}'\frac{f(\boldsymbol{r},\boldsymbol{p})f(\boldsymbol{r},\boldsymbol{p}')}{1+[(\boldsymbol{p}-\boldsymbol{p}')/\mu_k]^2}\ . \tag{2}$$

$f(\boldsymbol{r},\boldsymbol{p})$ is the phase space distribution function whose integral over $\boldsymbol{p}$ is normalized to the density $\rho(\boldsymbol{r})$. At zero temperature and for uniform density, we can carry out the integral in Eqs. (1) and (2) [7].

By choosing parameters $\alpha, \beta, C_{\rm ex}^{(k)}$, and $\mu_k (k = 1, 2)$ appropriately, we can fit the saturation density ρ_0 and the binding energy per nucleon as well as the real part of the global optical potential of Hama et al. [41], for a given value of γ. The parameter sets in Table 1 fulfill the saturation properties [33, 34]. The abbreviation "Sky" is the momentum independent parameter sets, and "Sky+mom" contains both density and momentum dependent parts. For momentum dependence, we adopt the parameters in Ref. [38] with some modification. For details, one can refer to Refs. [1, 35, 36, 37, 38].

We have introduced the above mean-field into JAM [25] by means of RQMD/S [26] frame work. The Relativistic Quantum Molecular Dynamics (RQMD) is a constraint Hamiltonian dynamics, in which we can treat the mean-field in a covariant way. While covariant equation of motion should have $8N$ phase space variables, (q^μ, p^μ), the number of actual dynamical variables is $6N$, $(\boldsymbol{r},\boldsymbol{p})$. Then we need $2N$ constraints [39]. In RQMD, we set N on mass shell constraints and N time-fixation constraints. We

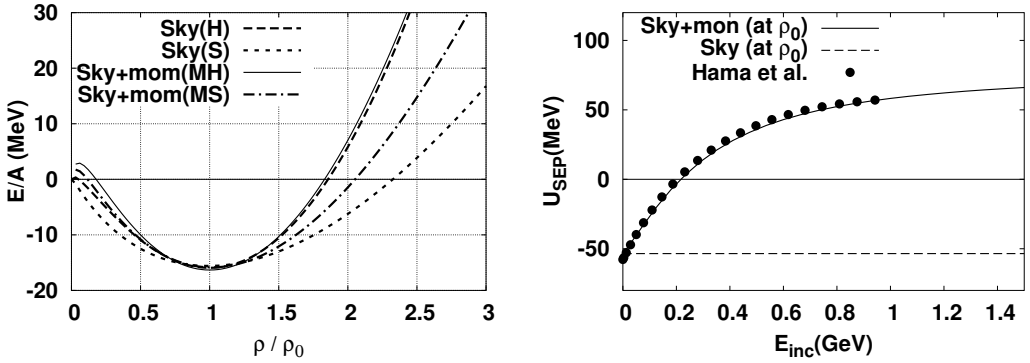

Figure 1: Left: Density dependence of EOS in Eq. (2). Two-potentials are shown, which is momentum–independent "Sky" [34] and -dependent "Sky+mom' . We can see they saturate at $\rho = \rho_0$. Right: Momentum dependence of potential in Eq.(1). Parameter sets of "Sky+mom" are described, also momentum-independent sets "Sky" are shown. It reproduces the form of real part of optical potential taken from Hama [41] fitted the range of $1 \lesssim E_{\rm inc} \lesssim 1000$ MeV with assuming uniform nuclear matter.

Type	α (MeV)	β (MeV)	γ	$C_{\rm ex}^{(1)}$ (MeV)	$C_{\rm ex}^{(2)}$ (MeV)	μ_1 (fm^{-1})	μ_2 (fm^{-1})	K (MeV)
Sky (H) [33]	-124	70.5	2	—	—	—	—	380
Sky (S) [33]	-356	303	7/6	—	—	—	—	200
Sky+mom(MH)	-33	110	5/3	-277	663	2.35	0.4	448
Sky+mom(MS)	-268	345	7/6	-277	663	2.35	0.4	314

Table 1: Parameter set of density-dependent and momentum-independent/dependent potential.

follow the work by Maruyama et al. (RQMD/S) [26] for time fixation constraints, which is much simpler and more practical than the original RQMD time fixation [29, 30, 31].

$$\phi_i \equiv \begin{cases} H_i \equiv p_i^2 - m_i^2 c^2 - 2m_i V_i \approx 0 & (i = 1, \ldots, N) \ , \\ \chi_{i-N} \equiv \hat{a} \cdot (q_{i-N} - q_N) \approx 0 & (i = N+1, \ldots, 2N-1) \ , \\ \chi_N \equiv \hat{a} \cdot q_N - \tau \approx 0 & (i = 2N) \ . \end{cases} \tag{3}$$

The symbol "$\approx$" is the weak equality initiated by Dirac [40]. Here, $\hat{a}$ is 4-component vector corresponding to $(1, \mathbf{0})$ at the reference frame, and q_i represents the time-space coordinates of the i-th particle.

By requiring that $2N$ constants are kept in time, Lagrange multipliers u_i are obtained, then we get the Hamiltonian and the equation of motion as

$$H = \sum_{i=1}^{2N-1} u_i \phi_i \approx \sum_{j=1}^{N} \frac{1}{2p_j^0} (p_j^2 - m_j^2 - 2m_j V_j) \ , \tag{4}$$

$$\frac{d\boldsymbol{r}_i}{d\tau} \approx -\frac{\partial H}{\partial \boldsymbol{p}_i} = \frac{\boldsymbol{p}_i}{p_i^0} + \sum_{j=1}^{N} \frac{m_j}{p_j^0} \frac{\partial V_j}{\partial \boldsymbol{p}_i} \ , \quad \frac{d\boldsymbol{p}_i}{d\tau} \approx \frac{\partial H}{\partial \boldsymbol{r}_i} = -\sum_{j=1}^{N} \frac{m_j}{p_j^0} \frac{\partial V_j}{\partial \boldsymbol{r}_i} \ . \tag{5}$$

The sum of the potential V_i becomes the total potential V, which is approximated in the actual calculation as

$$V = \sum_i V_i \simeq \sum_i \left[\left(\frac{\alpha \langle \rho_i \rangle}{2\rho_0} + \frac{\beta \langle \rho_i \rangle^\gamma}{(1+\gamma)\rho_0^\gamma} \right) + \sum_{k=1}^{2} \frac{C_{\rm ex}^{(k)}}{2\rho_0} \sum_{j(\neq i)} \frac{\rho_{ij}}{1 + [\tilde{\boldsymbol{p}}_{ij}/\mu_k]^2} \right] \ , \tag{6}$$

where $\langle \rho_i \rangle$ is the density averaged over the Gaussian packet of the i-th particle, and ρ_{ij} is the density overlap of the i-th and j-th packets. In evaluating the potential, we have used the covariant squared distance and relative momentum,

$$\tilde{\boldsymbol{r}}_{ij}^2 = -q_{ij}^2 + (q_{ij} \cdot P_{ij})^2 / P_{ij}^2 \ , \quad \tilde{\boldsymbol{p}}_{ij}^2 = -p_{ij}^2 + (p_{ij} \cdot P_{ij})^2 / P_{ij}^2 \ , \tag{7}$$

where $q^\mu_{ij} = q_i - q_j$, $p^\mu_{ij} = p_i - p_j$, $P^\mu_{ij} = p_i + p_j$. These variables, $\tilde{\boldsymbol{r}}^2_{ij}$ and $\tilde{\boldsymbol{p}}^2_{ij}$, represent the (squared) distance and relative momentum in the CM frame of the two particles.

We have combined the two important features described above, hadron-string cascade and mean-field, based on the cascade model, JAM. The effects of the mean-field in high-energy heavy-ion collisions are visible but not very large in the single particle spectra, as the rapidity distribution dN/dy or the transverse mass distribution $d^2N/m_T dm_T dy$. In the next section, we demonstrate that the mean-field effects are essential in anisotropic collective flows.

3 Collective Flows from SIS to SPS energies

When two heavy nuclei collide at high energies, copious hadrons are produced in the multiple scattering of hadrons. In the first chance and in the proceeding several collisions, hadrons are formed and propagate in dense matter, whose property is expected to affect the final hadron spectra. Especially, when the impact parameter is finite, pressure gradient is anisotropic in the initial stage of collision and it generates the particle anisotropy, called anisotropic flow.

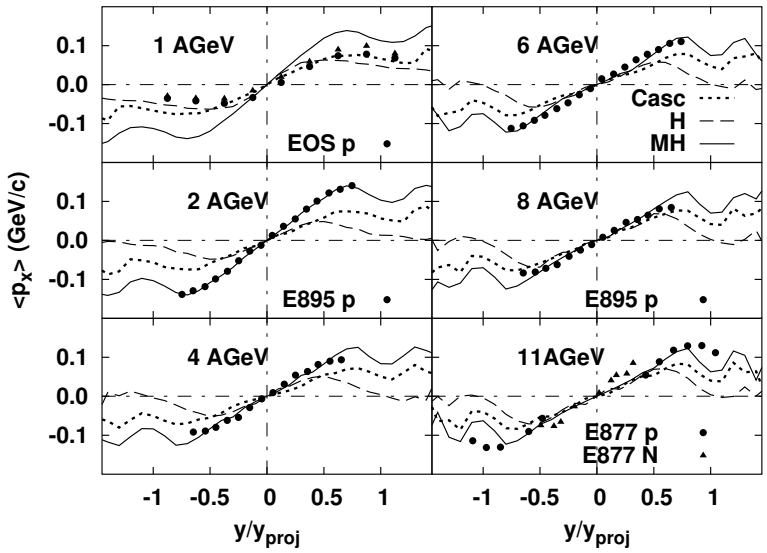

Figure 2: Sideward flow $\langle p_x \rangle$ of protons in AGS energy heavy-ion (Au+Au) collisions. We choose semi-central collisions $4 < b < 8$ fm. Dotted, dashed and solid lines show the results of Cascade, Cascade with "Sky"(H) mean-field and Cascade with "Sky+mom"(MH) mean-field, respectively. We see that "Sky + mom" gives a good description of experimental data for incident energies of $2 \leq E_{\rm inc} \leq 11$ A GeV. Experimental data are taken from Bevalac [13], AGS-E877 [17] and AGS-E895 [19].

Up to now, several kinds of collective flows are proposed as a probe of high density matter. The first one is called sideward flow, which is defined as the slope of the mean-value of p_x (in the direction of impact parameter) as a function of the rapidity,

$$F = \left. \frac{d\langle p_x \rangle}{d(y/y_{\rm proj})} \right|_{y=y_{\rm c.m.}} . \tag{8}$$

The sideward flow is generated by the participant-spectator interaction. Nucleons in the projectile nucleus feels repulsive interaction at high energies from the target nucleus during the contact time of projectile and target. This repulsion pushes nucleons out in the sideward direction giving positive sideward flow if the contact time is long enough. When the incident energy is very high, contact time becomes short mainly due to the Lorentz contraction, and the sideward flow decreases.

Figure 2 shows the incident energy dependence of sideward flow from SIS to AGS energies. Data tell us that the sideward flow first increases as a function of the incident energy, reaches maximum at around $E_{\rm inc} \sim 2A$ GeV, and decreases above $2A$ GeV. Calculated results with Cascade (JAM without mean-field) do not reproduce this incident energy dependence. In Fig. 2, we find that cascade results in similar $\langle p_x \rangle$ behavior, giving small values of F and small incident energy dependence of the sideward flow. When repulsive mean-field effects are taken into account (JAM-RQMD/S), the sideward flow becomes stronger and has clear energy dependence. At the incident energies of $1 - 2A$ GeV, contact time is long enough and there is a significant effects of the mean-field on F. At higher incident energies, the mean-field effects become smaller, and the difference is almost negligible at the top AGS energy (11 A GeV) for F. However, we still find some differences in the $\langle p_x \rangle$ values at projectile and target rapidity region ($y/y_{\rm proj} \simeq \pm 1$), and the momentum dependent mean-field improves the description.

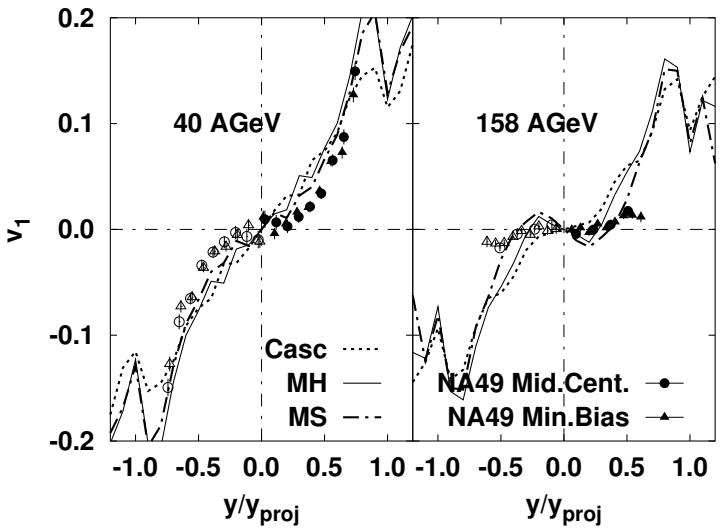

Figure 3: Directed flow v_1 of protons for SPS energy heavy-ion (Pb+Pb) collisions. Dotted, solid, and dot-dashed lines show the results of Cascade, Cascade with "Sky+mom"(MH) mean-field and Cascade with "Sky+mom"(MS) mean-field, respectively. Experimental data are taken from SPS-NA49 [23].

At SPS energies ($E_{\rm inc} = 40, 158A$ GeV), the directed flow (v_1) is measured instead of $\langle p_x \rangle$ as a function of the rapidity. Here v_n is defined as the n-th Fourier coefficient,

$$\frac{d^3N}{p_T dp_T dy d\phi} = \frac{d^2N}{2\pi p_T dp_T dy} \times \left(1 + \sum_n 2v_n(p_T, y) \cos n\phi \right) , \tag{9}$$

$$v_1 = \langle \cos\phi \rangle = \left\langle \frac{p_x}{p_T} \right\rangle , \quad v_2 = \langle \cos 2\phi \rangle = \left\langle \frac{p_x^2 - p_y^2}{p_T^2} \right\rangle , \quad \ldots \tag{10}$$

where the azimuthal angle ϕ is measured from the reaction plane. These Fourier coefficients are easier to measure since no particle identification is necessary. These collective flows are reviewed in Ref. [28].

In Fig. 3, we compare the calculated results with the data of Pb+Pb collisions at $E_{\rm inc} = 40$ and 158 A GeV [23]. The values of v_1 data are of the order of a few percents, which are smaller than the values expected at AGS energies. In addition, the rapidity dependence of data is much more flatter than that in the Cascade results. Contrary to $\langle p_x \rangle$ at AGS energies, mean-field suppresses v_1 at SPS, which is the direction to be closer to the data behavior. This tendency may be understood by the time scale. Since the projectile and target pass through in a very short time due to the large Lorentz contraction factor at SPS, the pressure effects would be in the reverse direction.

While the mean-field effects in v_1 are still visible even at SPS energies, the short participant-spectator interaction time makes the collective sideward flow signal smaller. Thus at SPS and RHIC, the next Fourier coefficient, called as the elliptic flow (v_2), has been discussed more extensively. The participants form an almond-like shape in the transverse plane after the spectators go through, and actual participant dynamics would emerge at mid-rapidities. If the participants are well thermalized, the pressure gradient

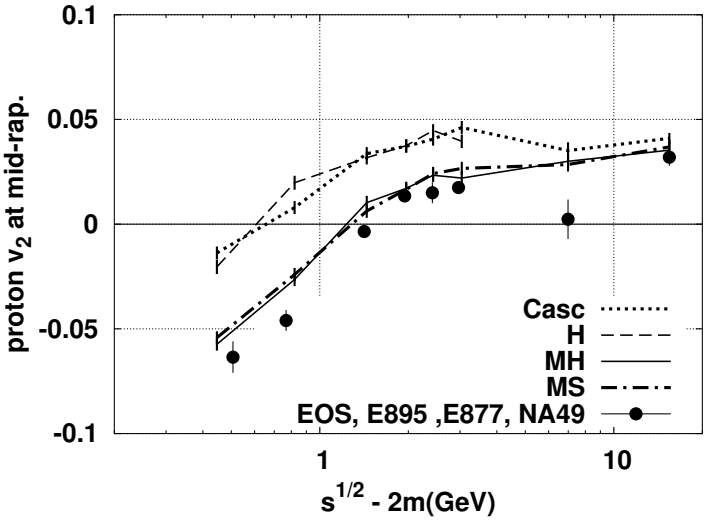

Figure 4: Incident energy dependence of nucleon elliptic flow at mid-rapidities ($-0.2 < y/y_{\rm proj} < 0.2$) in semi-central ($4 < b < 8$ fm) heavy-ion collisions from 1 A GeV to 160 A GeV. Dotted, dashed, solid, and dot-dashed lines show the results of Cascade, Cascade with "Sky"(H) mean-field, Cascade with "Sky+mom"(MH) mean-field and Cascade with "Sky+mom"(MS) mean-field, respectively. The experimental data are taken from LBL-EOS, AGS-E895, E877 [18] and SPS-NA49 [23].

is stronger in the x (shorter axis of the almond) direction, leading to the enhancement of in-plane particle emission, i.e. positive v_2. At lower energies ($E_{\rm inc} \lesssim 4A$ GeV), we find squeezing ($v_2 < 0$) of nucleons during the contact of projectile and target rather than the pure participant expansion. The elliptic flow, therefore, shows the strength of the repulsive interaction at lower energies and how much pressure is constructed at higher energies.

In Fig. 4, we show the incident energy dependence of proton v_2 at mid-rapidities. Experimental data clearly show the evolution from squeezing to almond shaped participant dynamics. In Cascade, we cannot explain strong squeezing effects at lower energies, and the calculated v_2 values are generally larger than data at all the incident energies investigated here. Momentum dependent mean-field, which is repulsive in the energy range under consideration, pushes down the elliptic flow significantly. We can qualitatively reproduce the incident energy dependence from SIS to SPS energies, except for the data at $E_{\rm inc} = 40A$ GeV. For the data at $E_{\rm inc} = 40A$ GeV, the extracted v_2 value strongly depends on the analysis; we have adopted the value of the reaction plane analysis, but it becomes much larger if we adopt the value extracted in particle correlation method [23]. Confirmation of data is necessary to examine the incident energy dependence of v_2, whether it is a monotonic function or has a dip at around $E_{\rm inc} \sim 40A$ GeV [23].

4 Summary

We have investigated collective flows in heavy-ion collisions from SIS (1 A GeV), AGS ($2-11A$ GeV) to SPS (158 A GeV) energies by using a combined framework of hadron-string cascade (JAM) [25] and covariant constraint Hamiltonian dynamics (RQMD/S) [26]. In hadron-string cascade, various particle production mechanisms are taken into account — production and decay of resonances and strings, and jet production and its fragmentation, while partonic interaction has only a minor role up to SPS energies. Momentum dependence of the mean-field is fitted to the real part of the Schrödinger equivalent global optical potential of Hama et al. [41]. Saturation properties are fitted by introducing the density dependent potential of Skyrme-type in the power series of ρ, $U(\rho) = \alpha(\rho/\rho_0) + \beta(\rho/\rho_0)^\gamma$. Calculated results of Cascade, Cascade with momentum dependent mean-field, and Cascade with momentum independent mean-field are compared with the data of sideward ($\langle p_x \rangle$), directed (v_1), and elliptic (v_2) flows from SIS to SPS energies. Generally, results with momentum dependent mean-field reasonably well explain the trend of data. Specifically, we cannot reproduce strong enhancement of the sideward flow at around

$E_{\rm inc} = 2A$ GeV, strong squeezing seen in v_2 for $E_{\rm inc} \lesssim 4A$ GeV, and suppression of v_1 at $E_{\rm inc} = 158A$ GeV, without momentum dependent mean-field. The present analysis then extends the work by Sahu et al. [24] and Danielewicz et al. [10] in the incident energy range, implying that our current knowledge — hadron-string cascade in momentum dependent mean-field — is consistent with the observed collective behavior in heavy-ion collisions.

There are still many problems to pin down the equation of state (EOS) of dense nuclear matter from the heavy-ion data. First, we have considered the mean-field only for nucleons in this work, and the mean-field for resonance hadrons and mesons such as Δ, Λ and kaons are ignored. This prescription significantly reduces the density used in evaluating the mean-field at high energies, and it may lead to the underestimate of the density dependent part of the mean-field effects. Since we already have the flow data for Λ, π and kaons, it would be possible to extend the present work to include and to discuss the mean-field effects for other hadrons than nucleons. Secondly, the functional form of the mean-field may be problematic. When the momentum dependence is fitted in the Lorentzian form, the EOS necessarily becomes relatively stiff, as shown in Table 1, in the Skyrme-type form. The small sensitivity on EOS with momentum dependence appeared in this work may be suggesting that the probed EOS range is not wide enough. Thirdly, more detailed theoretical analyses such as the impact parameter, p_T, and particle dependence of flows with higher simulation statistics would be desired. Works in these directions are in progress.

This work is supported in part by the Ministry of Education, Science, Sports and Culture, Grand-in-Aid for Scientific Research (C)(2), No. 15540243, 2003.

References

[1] G. F. Bertsch and S. Das Gupta, Phys. Rep. **160** (1988), 189.

[2] S. Aoki *et al.*(JLQCD Collab.) Nucl. Phys. Proc. Suppl. **73** (1999), 459.

[3] J. Kapusta and D. Strottman, Phys. Lett. B **106** (1981), 33.

[4] H. Stöcker *et al.*, Phys. Rev. C **25** (1982), 1873.

[5] H. A. Gustafsson *et al.*, Phys. Rev. Lett. **52** (1984), 1590.

[6] H. Kruse, B. V. Jacak and H. Stöcker, Phys. Rev. Lett. **54** (1985), 289.

[7] G. M. Welke *et al.*, Phys. Rev. C **38** (1988), 2101.

[8] L. P. Csernai, G. Fai, C. Gale, and E. Osnes, Phys. Rev. C **46** (1992), 736.

[9] P. Danielewicz, Nucl. Phys. **A 673** (2000), 375.

[10] P. Danielewicz, R. Racey, W. G. Lynch, Science **298**,(2002), 1592.

[11] P. Chung *et al.* (E895 Collab.) and P. Danielewicz, Phys. Rev. C **66** (2002), 021901(R).

[12] J. Chance *et al.* (EOS Collab.), Phys. Rev. Lett. **78** (1997), 2535.

[13] J. C. Kinter *et al.*, Phys. Rev. Lett. **78** (1997), 4165.

[14] K. G. R. Doss *et al.*, Phys. Rev. Lett. **57** (1986), 302.

[15] N. Bastid *et al.* (FOPI Collab.), Nucl. Phys. **A 622** (1997), 573.

[16] A. Andronic *et al.* (FOPI Collab.), Phys. Rev. C **67** (2003), 034907.

[17] J. Barrette *et al.* (E877 Collab.), Phys. Rev. C **56** (1997), 1420, *ibid.* 3254.

[18] C. Pinkenburg *et al.* (E895 Collab.), Phys. Rev. Lett. **83** (1999), 1295.

[19] H. Liu *et al.* (E895 Collab.), Phys. Rev. Lett. **84** (2000), 5488.

[20] J. L. Klay *et al.* (E895 Collab.), Phys. Rev. Lett. **88** (2002), 102301.

[21] H. Appelshäuser *et al.* (NA49 Collab.), Phys. Rev. Lett. **80** (1998), 4136.

[22] H. Appelshäuser *et al.* (NA49 Collab.), Phys. Rev. Lett. **82** (1999), 2471.

[23] C. Alt *et al.* (NA49 Collab.), Phys. Rev. C **68** (2003), 034903.

[24] P.K. Sahu, W. Cassing, U. Mosel and A. Ohnishi, Nucl. Phys. **A 672** (2000), 376.

[25] Y. Nara, N. Otuka, A. Ohnishi, K. Niita, and S. Chiba, Phys. Rev. C **61** (2000),024901.

[26] T. Maruyama *et al.*, Prog. Theor. Phys. **96** (1996), 263.

[27] X. -N. Wang and M. Gyulassy, Phys. Rev. D **44** (1991), 3501.

[28] J. -Y. Ollitrault, Nucl. Phys. **A 638** (1998), 195c. Nucl. Phys. **A 698** (2002), 479c.

[29] H. Sorge, H. Stöcker and W. Greiner, Ann. of Phys.**192** (1989), 266.

[30] H. Sorge, Phys. Rev. C **52** (1995), 3291.

[31] T. Maruyama *et al.*, Nucl. Phys. **A 534** (1991), 720.

[32] T. Sjöstrand *et al.*, Comp. Phys. Comm. **135** (2001),238.

[33] J. Aicherin and H. Stöcker, Phys. Lett. B **176** (1986), 14.

[34] J. Aicherin *et al.*, Phys. Rev. Lett. **58** (1987), 1926.

[35] L. P. Csernai, Introduction to Relativistic Heavy Ion Collisions, JHON WILEY & SONS (1994).

[36] Y. Hirata *et al.*, Nucl. Phys. **A 707** (2002),193; Y. Hirata, Ph.D. thesis, Hokkaido University (2000).

[37] K. Niita, Jaeri-Conf 1996-009, 22.

[38] T. Maruyama, K. Niita, T. Marutama, S. Chiba and A. Iwamoto, Phys. Rev. C **57** (1998), 655.

[39] A. Komar, Phys. Rev. D **18** (1978), 1881, 1887, 3617.

[40] P. A. M. Dirac, Rev. of Mod. Phys. **21** (1949), 392.

[41] S. Hama *et al.*, Phys. Rev. C **41** (1990), 2737.